

Image Restoration After Pixel Binning in Image Sensors*

LI Hao (李昊), ZHANG Hui (张辉), GUO Xiaolian (郭晓莲), HU Guangshu (胡广书)**

Department of Biomedical Engineering, Tsinghua University, Beijing 100084, China

Abstract: A method was developed to restore degraded images to some extent after the pixel binning process in image sensors to improve the resolution. A pixel binning model was used to approximate the original un-binned image. Then, the least squares error criterion was used as a constraint to reconstruct the restored pixel values from the binning model. The technique achieves about a one-decibel increase in the peak signal-to-noise ratio compared with the original estimated image. The technique has good detail preservation performance as well as low computation load. Thus, this restoration technique provides valuable improvements in practical, real time image processing.

Key words: image restoration; image sensors; pixel binning

Introduction

Image sensors are widely used to acquire digitalized images. Real-time image acquisition often uses pixel binning to reduce decreases of the signal-to-noise ratio (SNR)^[1-6]. However, the pixel binning process does degrade the original image, which can be restored to some extent. The fact that pixels from the image sensor are binned from the original un-binned pixels can be used to help the restoration. Thus, a higher resolution image can be restored from the binned image.

1 Pixel Binning

Image sensors, which are in essence transducers, convert photons into electrical signals. As the photons fall onto the surface of the image sensors, electrons accumulate in each pixel. Once the exposure is finished, the charges are transferred to the output and digitized. Most image sensors have the ability to combine multiple pixel charges with one single large pixel, which

represents all the individual pixels contributing to the charge. This is referred to as binning. No-binning or 1×1 binning means the individual pixels are retained. With 2×2 binning, four adjacent pixels are binned into one larger pixel and read out. With this option, the light sensitivity is increased four times from the four-pixel contribution; however, the image resolution is reduced by half. The diagram in Fig. 1 illustrates the pixel-binning process for no-binning, 2×2 binning, and 3×3 binning.

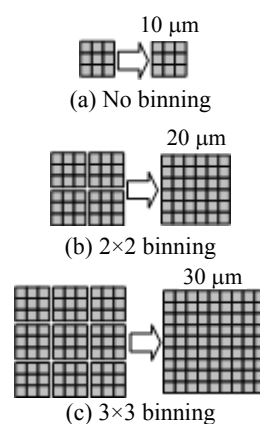


Fig. 1 Diagram for pixel-binning

The pixel binning technique is helpful for image acquisition. One primary benefit of binning is a higher SNR in the readout signal. With no binning, the

Received: 2008-05-20; revised: 2009-03-16

* Supported by the National Key Basic Research and Development (973) Program of China (No. 2006CB705700)

** To whom correspondence should be addressed.

E-mail: hgs-dea@mail.tsinghua.edu.cn; Tel: 86-10-62784568

readout noise is added during each readout and will be added to each individual pixel. However, in the binning mode, the noise is added to the binned pixel which has the combined signal from multiple individual pixels^[7-12]. Ideally, this operation can produce an SNR improvement equal to the binning factor, which equals four with 2×2 binning.

Another benefit of binning is to increase the readout frame rate. Since the bottleneck in the readout is the pixel digitization, the binning technique can be used to effectively increase the total frame rate of a given system. Highly binned low-resolution images can be read out very fast when high speed is needed^[2,6,13].

According to the sampling theory, images acquired from image sensors can be viewed as digitized discrete samples from the original continuous two-dimensional signal. However, the pixel binning process does not follow this sampling procedure. In Fig. 2, the triangular dots represent the original samples and the circular dots represent the binned image with 2×2 binning. Each binned image pixel represents the area of four adjacent sub-areas. The binned value is equal to the summation of the four adjacent individual pixels rather than the sample at the position of the continuous signal. Pixel binning then degrades image resolution. However, the binned image can be restored to acquire an image with higher resolution. Though the pixel binning process can not be completely reversed, proper restoration can give a good approximation of the original image, which is generally valuable in image acquisition.

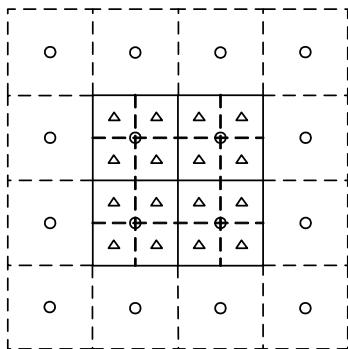


Fig. 2 Diagram for the image sample and pixel-binning

2 Method

For simplicity, we consider only 2×2 binning. The idea can be directly extended to larger-scale binning. To clearly explain the idea, we first explain some of the

terms used in the derivation.

A 2×2 binned image is acquired from the detector. Let $I(m, n)$ denote the binned image, where $m = 1, 2, \dots, M$ and $n = 1, 2, \dots, N$. The binned image can be considered to be acquired from the original un-binned image $I_O(i, j)$, where $i = 1, 2, \dots, 2M$ and $j = 1, 2, \dots, 2N$. Since the pixel binning can not be completely reversed, the restored image $I_R(i, j)$ can be a good approximation of $I_O(i, j)$. The restored image $I_R(i, j)$ follows the binning procedure which can be modeled by a very simple equation as follows:

$$I(m, n) = (I_R(2m - 1, 2n - 1) + I_R(2m, 2n - 1) + I_R(2m - 1, 2n) + I_R(2m, 2n)) / 4 \quad (1)$$

However, Eq. (1) has an infinite number of solutions and $I_R(i, j)$ cannot be obtained without additional information and constraints. To restore the binned image, we first get an estimate of $I_O(i, j)$, which can be denoted as $I_E(i, j)$. Then, we need to find $I_R(i, j)$ which best approximates $I_O(i, j)$. However, since the real values $I_O(i, j)$ cannot be obtained, we substitute $I_E(i, j)$ for $I_O(i, j)$ to find the best approximation. A simple, meaningful constraint for each binned pixel (m_0, n_0) is

$$\min \sum_{i=2m_0-1}^{2m_0} \sum_{j=2n_0-1}^{2n_0} (I_R(i, j) - I_E(i, j))^2 \quad (2)$$

The estimation $I_E(i, j)$ does not necessarily need to follow the pixel binning model in Eq. (1). There are many ways to obtain this estimation, e.g., the interpolated image of $I(m, n)$, which is widely used in image processing to acquire enlarged images^[14].

The constraint in Eq. (2) is a least square error (LSE) criterion, which enables analytic solution to Eq. (1). The Lagrange multiplier method can be used to form a new function to find the minimum of

$$\sum_{i=2m_0-1}^{2m_0} \sum_{j=2n_0-1}^{2n_0} (I_R(i, j) - I_E(i, j))^2$$

for each binned pixel (m_0, n_0) subject to

$$\sum_{i=2m_0-1}^{2m_0} \sum_{j=2n_0-1}^{2n_0} I_R(i, j) - 4I(m_0, n_0) = 0.$$

Therefore,

$$F(m_0, n_0) = \sum_{i=2m_0-1}^{2m_0} \sum_{j=2n_0-1}^{2n_0} (I_R(i, j) - I_E(i, j))^2 - \lambda \left(\sum_{i=2m_0-1}^{2m_0} \sum_{j=2n_0-1}^{2n_0} I_R(i, j) - 4I(m_0, n_0) \right) \quad (3)$$

where $F(m_0, n_0)$ is the Lagrangian function and the constant λ is the Lagrange multiplier.

Taking partial derivatives of Eq. (3) gives four equations for the four pixels $(2m_0-1, 2n_0-1)$, $(2m_0, 2n_0-1)$, $(2m_0-1, 2n_0)$, and $(2m_0, 2n_0)$.

$$\begin{aligned} 2(I_R(i_0, j_0) - I_E(i_0, j_0)) - \lambda &= 0, \\ i_0 = 2m_0 - 1, 2m_0; \quad j_0 = 2n_0 - 1, 2n_0 \end{aligned} \quad (4)$$

So we have

$$\begin{aligned} I_R(i_0, j_0) &= \frac{\lambda}{2} + I_E(i_0, j_0), \\ i_0 = 2m_0 - 1, 2m_0; \quad j_0 = 2n_0 - 1, 2n_0 \end{aligned} \quad (5)$$

According to Eq. (1), for each binned pixel (m_0, n_0) ,

$$2\lambda + \sum_{i=2m_0-1}^{2m_0} \sum_{j=2n_0-1}^{2n_0} I_E(i, j) = 4I(m_0, n_0) \quad (6)$$

Then

$$\lambda = \frac{4I(m_0, n_0) - \sum_{i=2m_0-1}^{2m_0} \sum_{j=2n_0-1}^{2n_0} I_E(i, j)}{2} \quad (7)$$

We then substitute Eq. (7) for λ into Eq. (5) to obtain the restored pixel values at $(2m_0-1, 2n_0-1)$, $(2m_0, 2n_0-1)$, $(2m_0-1, 2n_0)$, and $(2m_0, 2n_0)$:

$$\begin{aligned} I_R(i_0, j_0) &= \frac{4I(m_0, n_0) - \sum_{i=2m_0-1}^{2m_0} \sum_{j=2n_0-1}^{2n_0} I_E(i, j)}{4} + I_E(i_0, j_0), \\ i_0 = 2m_0 - 1, 2m_0; \quad j_0 = 2n_0 - 1, 2n_0 \end{aligned} \quad (8)$$

Now we are able to get the values of the restored image pixels $I_R(i, j)$ in terms of the estimated values. A flow chart is given in Fig. 3 to better illustrate the method. All the additional work in the method is simply to make corrections to the pixels after the estimation. The calculational load, as shown in Eq. (8), is very small.

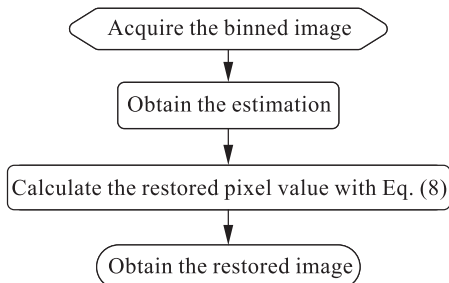


Fig. 3 Flow chart

3 Geometric Description

The geometric description of the process is given to

provide a profound understanding of the method. Only the one-dimensional case is shown without loss of generality to explain the concept. The description here can be directly extended to the two-dimensional case for an image.

The estimation method used here is bilinear interpolation, which is linear interpolation in the one-dimensional case. The continuous light solid line shown in Fig. 4 indicates the original continuous signal. The original signals are sampled at the sampling frequency, indicated by the vertical dashed grid. The sampled signals are then binned and read out, as indicated by the heavy solid points $I(n-1)$, $I(n)$, $I(n+1)$, and $I(n+2)$. The binned signal is interpolated to acquire the signals at the original sampling frequency. Using linear interpolation on the resampling grid indicated in Fig. 4, we have

$$\begin{aligned} I_E(2n-1) &= \frac{1}{4}I(n-1) + \frac{3}{4}I(n), \\ I_E(2n) &= \frac{3}{4}I(n) + \frac{1}{4}I(n+1) \end{aligned} \quad (9)$$

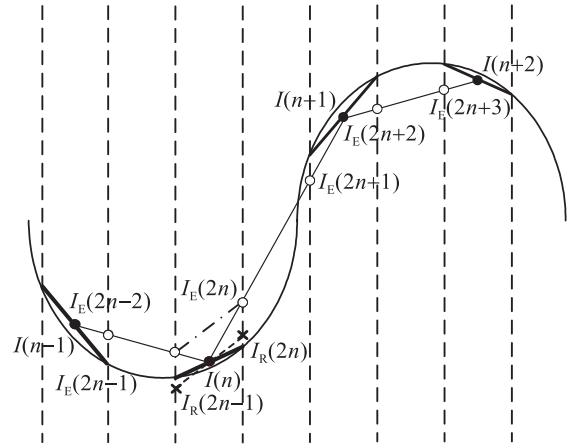


Fig. 4 Diagram of the method in one dimension

The dotted dashed line between $I_E(2n-1)$ and $I_E(2n)$ depicts the profile of the interpolated signal which deviates greatly from the original profile and does not pass through the binned signal $I(n)$. The correction to the interpolated signals gives

$$\begin{aligned} I_R(2n-1) &= -\frac{1}{8}I(n-1) + I(n) + \frac{1}{8}I(n+1), \\ I_R(2n) &= \frac{1}{8}I(n-1) + I(n) - \frac{1}{8}I(n+1) \end{aligned} \quad (10)$$

The dashed line between $I_R(2n-1)$ and $I_R(2n)$, indicated by \times , passes through the binned signal $I(n)$ and is a better linear approximation to the

original profile. The fact that the readout signal is obtained through binning is an important part of the method.

4 Simulation Results

The method is evaluated quantitatively using the classic fishing boat image comparing interpolation and the proposed method. The original boat image, which is 512×512 pixels, was first binned into a 256×256 pixel image. Bilinear interpolation was used to acquire the estimated image. Then, the estimated image was corrected to acquire the restored image.

The peak signal-to-noise ratio (PSNR) is used to evaluate the image quality. The PSNR is defined as

$$\text{PSNR} = 10 \cdot \lg \left(\frac{255^2}{\text{MSE}} \right),$$

$$\text{MSE} = \frac{1}{mn} \sum_{i=0}^{m-1} \sum_{j=0}^{n-1} |I(i, j) - K(i, j)|^2 \quad (11)$$

where m and n are the numbers of rows and columns in image I or K .

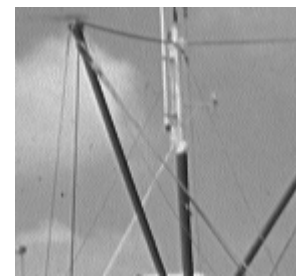
The PSNRs for the bilinear-interpolated and the restored images are listed in Table 1. The detail-preserving ability of the method was evaluated using part of a boat, which contains fine details cropped from the original image. The PSNRs for this part were also listed in Table 1. The results in Table 1 show that the restoration process has improved the image quality in terms of the PSNR with more than one decibel improvement between the overall or partial PSNRs of the interpolated and restored images. Thus, the corrected image is a better approximation to the original signal than the estimate, i.e., the interpolated image, since the restored image rather than the interpolated image utilizes the pixel binning model in Eq. (1).

Table 1 PSNRs of the interpolated and restored fishing boat image

		PSNR (dB)
Overall	Interpolated	29.06
	Restored	30.29
Partial	Interpolated	39.54
	Restored	40.64

The cropped boat images are shown in Fig. 5 to subjectively evaluate the method. The bilinear interpolation smears the fine details while the proposed restoration method helps to recover these fine details to some extent. Though the restoration is not perfect, the result

can be seen improved compared with the estimate.



(a)



(b)



(c)



(d)

Fig. 5 Part of boat image cropped from (a) the original image, un-binned, (b) the bilinear-interpolated image after pixel-binning, (c) the restored image from (b), and (d) the bicubic-interpolated image after pixel-binning

5 Discussion

This restoration method helps restore an image from a degraded binned image. The estimate, which might not follow the pixel binning model, provides a constraint to make the restoration possible. The restoration should strictly follow the pixel binning model as a better approximation to the original signal. This method uses

the LSE criterion as a constraint. The least absolute error (LAE) or the maximum norm could also be used as the constraint. However, if the LAE or the maximum norm is used as the constraint, no simple analytical solution can be derived for each point, so the image processing would not be practical.

Binned images from image sensors are generally enlarged to the original image when processed, e.g., directly interpolated for the enlargement. However, as stated in Section 2, this process does not utilize the pixel binning knowledge. The restoration method can then be considered a correction to the interpolation. The interpolation method in the restoration could vary from a very simple bilinear model to the more complex B-spline interpolation. Though the PSNR is not a reliable measurement to judge the image quality, restoration using simple interpolation as the estimation can give improved PSNR comparable to that of using more complex interpolation methods. For example, the current method with bilinear interpolation gives a PSNR of 30.29 dB. Bicubic interpolation with the interpolated boat image gives 30.11 dB. The bilinear-correction PSNR for the cropped part in Fig. 5 is 40.64 dB while the bicubic-interpolation gives a PSNR of 40.48 dB. The PSNRs for the counterparts are nearly equal. The bicubic-interpolated image is shown in Fig. 5d for comparison of the image quality. The current method can be seen to achieve comparable detail-preservation to the bicubic-interpolated image.

The calculational load for each point using bilinear-correction is significantly smaller than with bicubic-interpolation. For example, with 2×2 binning, bilinear interpolation requires four multiplications and three additions for each point. The correction process then requires only one division by four, one multiplication by four, and five additions. The division or multiplication by four can be implemented by a data shift when implemented in hardware, which is very fast. Therefore, the total calculational load for the bilinear-correction is just six multiplications, eight additions, and the data shift. The bicubic interpolation requires unavoidable 16 multiplications and 15 additions. Therefore, this method can give images with comparable PSNR with much less computational load.

6 Conclusions

An image restoration that receives the binning process

was developed to restore degraded images. The method is proven to be efficient and to provide good detail preservation. The method does not significantly increase the calculational load during implementation, which is valuable for real-time image processing.

References

- [1] Bock N E. Apparatus and method for pixel binning in an image sensor. U.S. Patent 7091466B2, Aug. 15, 2006.
- [2] Zhou Z, Pain B, Fossum E R. Frame-transfer CMOS active pixel sensor with pixel binning. *IEEE Trans. Electron Devices*, 1997, **44**: 1764-1768.
- [3] Yang G, Dosluoglu T. An image sensor having resolution adjustment employing an analog column averaging/row averaging for high intensity light or row binning for low intensity light. European Patent 1659776, 2006.
- [4] Guidash R M. Image sensor with charge binning. European Patent 1656799, 2006.
- [5] Yang G, Dosluoglu T. A column averaging/row binning circuit for image sensor resolution adjustment in lower intensity light environment. European Patent 1659778, 2006.
- [6] Guidash R. CMOS image sensor pixel with selectable binning. WO Patent WO/2006/130518, 2006.
- [7] Aach T, Schiebel U, Spekowius G. Digital image acquisition and processing in medical X-ray imaging. *J. Electronic Imaging*, 1999, **8**: 7-22.
- [8] Srinivas Y, Wilson D L. Quantitative image quality evaluation of pixel-binning in a flat-panel detector for X-ray fluoroscopy. *Med. Phys.*, 2004, **31**(1): 131-141.
- [9] Maolinbay M, El-Mohri Y, Antonuk L E, Jee K-W, Nassif S, Rong X, Zhao Q. Additive noise properties of active matrix flat-panel imagers. *Med. Phys.*, 2000, **27**(8): 1841-1854.
- [10] Matsuura N, Zhao W, Huang Z, Rowlands J A. Digital radiology using active matrix readout: Amplified pixel detector array for fluoroscopy. *Med. Phys.*, 1999, **26**(5): 672-681.
- [11] Jardin W D, Parks C, Doan H, Kurfiss N, Wetzel K. A large format, high-performance CCD sensor for medical X-ray applications. In: *Proceedings of SPIE: Medical Imaging*. San Diego, USA, 2000: 167-175.
- [12] Phillips W C, Stewart A, Stanton M, Naday I, Ingersoll C. High-sensitivity CCD-based X-ray detector. *J. Synchrotron Rad.*, 2002, **9**: 36-43.
- [13] Bigas M, Cabruja E, Forest J, Salvi J. Review of CMOS image sensors. *Microelectronics Journal*, 2006, **37**(5): 433-451.
- [14] Lehmann T M, Gonner C, Spitzer K. Survey: Interpolation methods in medical image processing. *IEEE Trans. Medical Imaging*, 1999, **18**: 1049-1075.